Double Sine-Gordon ratchet induced by excitation of an internal mode

C. R. Willis and M. Farzaneh
Department of Physics, Boston University, 590 Commonwealth Avenue, Boston, Massachusetts 02215, USA
(Received 19 February 2004; published 10 January 2005)

In a recent paper [Phys. Rev. E **69**, 056612 (2004)] we showed the symmetry analysis of Flach *et al.* [Phys. Rev. Lett. **88**, 184101 (2002)] which predicted the appearance of directed energy current in homogeneously spatially extended systems described by nonlinear field equations coupled to a heat bath in the presence of a correct choice for the time dependence of an external ac field, $E(t)$, was due to the excitation of an internal mode. Flach *et al.* applied their analysis to the sine-Gordon (SG) equation and verified the symmetry breaking numerically. In the SG case we showed the internal mode coupled to the center of the mass variable, $X(t)$, that caused the symmetry breaking was $\Gamma(t)$ the slope of the kink. We also found that the phonon dressing of the SG kink by the ac driver, $\chi(t)$, was necessary for the occurrence of a directed energy current in the SG equation. We show in the case of the double sine-Gordon (DSG) equation that the excitation of the internal mode, $R(t)$ (where $R(t)$ is the separation of the two subkinks that make up the DSG soliton), combined with the phonon dressing of the DSG soliton also causes a directed energy current.

DOI: 10.1103/PhysRevE.71.016604 PACS number(s): 05.45.Yv

I. INTRODUCTION

Recently Flach *et al.* [1–3] showed that an external ac field $E(t)$ with the correct properties would cause the appearance of persistent directed energy currents in homogeneous spatially extended systems described by nonlinear field equations such as nonlinear Klein-Gordon systems with nonzero topological charge connected to a heat bath. The example they chose was the sine-Gordon (SG) equation which they solved numerically. They also showed the persistence of directed energy currents in the Hamiltonian limit exposed to ac fields but decoupled from the heat bath. The authors of Ref. [1] suggested that the origin of the observed rectification in the underdamped limit was due to the nonadiabatic excitation of internal kink modes and their interaction with the translational kink motion.

In Ref. [4] we proved that the argument of Flach *et al.* [1–3] is correct for the SG equation using a rigorous collective variable (CV) theory for the nonlinear Klein-Gordon equations derived in Refs. [5,6]. We showed explicitly for the ac driver SG equation that the collective variable $X(t)$ and the slope $\Gamma(t)$ become time dependent and dynamically coupled to each other due to the phonon dressing caused by the ac field. As a consequence of the coupling of $X(t)$ and $\Gamma(t)$ caused by the phonon dressing, the ac driver SG equation has a directed energy current—i.e., a time inversion symmetry breaking.

In the double sine-Gordon (DSG) equation there is a second collective variable $R(t)$, which represents the separation of the two SG kinks that make up the DSG soliton which can serve as the internal kink mode that takes part in the symmetry breaking. In this paper we take the slope to be a constant and prove that the CV $R(t)$ combined with the phonon dressing causes rectification of the energy current in the DSG.

In Sec. II we derive the coupled equations of motion for $X(t)$ and $R(t)$ including the terms due to the dressing of the kink by phonons. We present our results for the solution of $X(t)$ and $R(t)$ and for the generation of directed energy currents in Sec. III. In Sec. IV we discuss our results.

II. DERIVATION OF CV EQUATIONS OF MOTION

We outline the derivation of the equations of motion for the collective variables $X(t)$ and $R(t)$ which are derived in detail in Refs. [5,6] for the DSG equation driven by an ac driver. The DSG equation in the presence of an ac driver and damping due to a heat bath is

$$\phi_{,tt} - \phi_{,xx} + \frac{\partial V(\phi)}{\partial \phi} = -\frac{\partial V_{\text{ext}}}{\partial \phi} - \beta\phi_{,t} + \eta(x,t), \qquad (1)$$

where $\beta\phi_{,t}$ represents the damping due to the heat bath and the Gaussian white noise η is characterized by the standard correlation function $\langle \eta(x,t)\eta(x',t')\rangle = 2\beta\gamma^{-1}\delta(x-x')\delta(t-t')$, where γ is the inverse temperature:

$$V(\phi) \equiv -4(2\pi/l_0)\text{sech}^2\,\mathcal{R} \times\left[(\cos\phi - 1)\sinh^2\mathcal{R} - \left(1 + \cos\frac{\phi}{2}\right)\right] \qquad (2)$$

and

$$V_{\text{ext}} \equiv (\epsilon_1\cos\omega t + \epsilon_2\cos[2\omega t + \theta])\phi \equiv f_1(t)\phi. \qquad (3)$$

Note that $f_1(t)$ is not shift symmetric as long as both ϵ_1 and ϵ_2 are nonzero. The parameters ϵ_1 and ϵ_2 represent the magnitude of the ac driver. We introduce the collective variables $X(t)$ and $R(t)$ by means of the ansatz

$$\phi = \sigma((2\pi/l_0)[x - X(t)], R(t)) + \chi((2\pi/l_0)[x - X(t)], R(t)), \qquad (4)$$

where σ is the solution of the unperturbed DSG which is

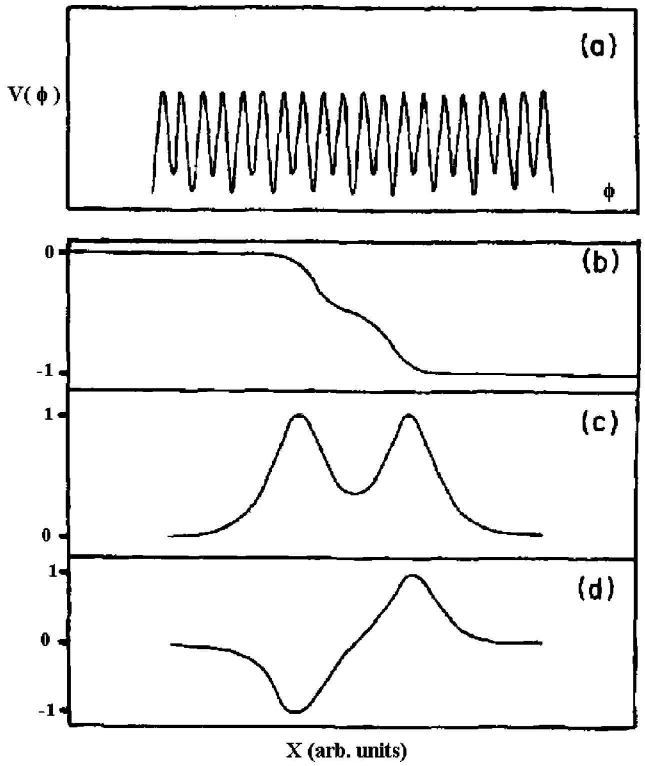

FIG. 1. (a) The DSG potential for $\mathcal{R} \geqslant 1.25$, (b) the solution to the unperturbed DSG equation, Eq. (5), for $X(0)=0$ and $R(0)=\mathcal{R}$, (c) the Goldstone mode $\partial\sigma/\partial X$ with $R(0)=\mathcal{R}$ and $X(0)=0$, and (d) $\partial\sigma/\partial R$, the approximate small oscillation function with $R(0)=\mathcal{R}$ and $X(0)=0$. Note that in the exact solution of the DSG with parameter $\mathcal{R}$, the distance between the subkinks that make up the DSG is $2\mathcal{R}$. Figure from Ref. [5].

$$\sigma((2\pi/l_0)[x-X(t)],R(t)) \equiv \sigma_{\rm SG}((2\pi/l_0)[x-X(t)]+R(t)) - \sigma_{\rm SG}(R(t)-(2\pi/l_0)[x-X(t)]) \tag{5}$$

and $\sigma_{\rm SG}(x)=4\tan^{-1}[\exp(x)]$ is the solution of the single SG equation. For convenience we reproduce, as our Fig. 1, Fig. (1) of Ref. [5] for $V(\phi)$, σ, $\partial\sigma/\partial X$, and $\partial\sigma/\partial R$. For the remainder of this paper we set the dimensionless parameter $(2\pi/l_0)$ equal to 1. In Ref. [4] we derived the dressing of the SG caused by $f_1(t)$. The result is

$$\chi_{\rm SG}(x) = \frac{4}{\pi} f(t) \mathrm{sech}^2\, x, \tag{6}$$

where

$$f(t) \equiv (\epsilon_1/2)\cos\omega t\left\{\frac{1-\omega}{\beta^2+(1-\omega)^2}+\frac{1+\omega}{\beta^2+(1+\omega)^2}\right\} + (\epsilon_2/2)\cos(2\omega t+\theta)\left\{\frac{1-2\omega}{\beta^2+(1-2\omega)^2} + \frac{1+2\omega}{\beta^2+(1+2\omega)^2}\right\}. \tag{7}$$

The dressing $\chi_{\rm DSG}$ to first order in ϵ_1 and ϵ_2 is

$$\chi_{\rm DSG} = \chi_{\rm SG}\{[x-X(t)]+R(t)\} - \chi_{\rm SG}\{R(t)-[x-X(t)]\} = (4/\pi)f(t)(\mathrm{sech}^2\{[x-X(t)]+R(t)\} - \mathrm{sech}^2\{[x-X(t)] - R(t)\}). \tag{8}$$

Since we increased the number of degrees of freedom by 2—namely, $X(t)$ and $R(t)$—it is necessary that $\chi_{\rm DSG}$ satisfy four constraints: namely,

$$C_X \equiv \int \sigma'_{\rm DSG}(y,R)\chi(y,t)dy = 0,$$

where $\sigma'_{\rm DSG}(y,R) \equiv \partial\sigma_{\rm DSG}(y,R)/\partial y$ and

$$C_R \equiv \int \sigma_{\rm R}(y,R)\chi(y,t)dy = 0,$$

where $\sigma_{\rm R}(y,R) \equiv \partial\sigma_{\rm DSG}(y,R)/\partial R$ and the same two constraints with χ replaced by Π, the momenta conjugate to χ. The constraints are used in obtaining the final equations of motion for $\ddot{R}$ and $\ddot{X}$. The details are given in Ref. [6].

We obtain the equations of motion for $\ddot{X}$ by multiplying Eq. (1) by $\partial\sigma/\partial X$ and integrating over X. The result given in Eq. (3.17) of Ref. [6] is

$$\frac{d}{dt}[M_X(R)(1-b_X)\dot{X}] = -\dot{X}\langle\sigma'|\partial\chi'/\partial t\rangle + \dot{X}\dot{R}\langle\sigma'_R|\chi'\rangle + f_1\int \sigma'(y)dy - \beta M_X\dot{X}, \tag{9}$$

where $y \equiv x-X(t)$ and where the dot product $\langle A|B\rangle \equiv \int_{-\infty}^{\infty} A(y,R)B(y,R)dy$. The explicit integrals of the various dot products in Eq. (9) are

$$M_X(R) \equiv \langle\sigma'|\sigma'\rangle = 8\left[1+\frac{2R}{\sinh 2R}\right], \tag{10}$$

$$\langle\sigma'|\partial\chi'/\partial t\rangle = \frac{16}{\pi}\dot{f}\int_{-\infty}^{\infty} d\mu\, \mathrm{sech}\,\mu\, \mathrm{sech}^2[2R-\mu]\tanh[2R-\mu], \tag{11}$$

$$\langle\sigma'|\chi'\rangle = \frac{16}{\pi} f\int_{-\infty}^{\infty} d\mu\, \mathrm{sech}\,\mu \times \tanh\mu\, \mathrm{sech}^2[2R-\mu]\tanh[2R-\mu], \tag{12}$$

$$b_X \equiv (M_X)^{-1}\langle\sigma''|\chi\rangle = -M_X^{-1}\langle\sigma'|\chi'\rangle. \tag{13}$$

Thus,

$$\dot{X}M_X\frac{\partial b_X}{\partial t} = \langle\sigma'|\partial\chi'/\partial t\rangle\dot{X}. \tag{14}$$

When we substitute Eq. (13) into Eq. (9) we obtain

$$\frac{d}{dt}[M_X(R)\dot{X}] \equiv \dot{P}_X = f\dot{X}\{-2\langle\sigma'|\chi'\rangle(\dot{f}/f) + \dot{R}\langle\sigma_R|\chi'\rangle\} - \beta P_X + 4\pi f_1, \tag{15}$$

where the momentum conjugate to X is $P_X \equiv M_X(R)\dot{X}$. In our units the energy current $J(t)$ is equal to $P_X(t)$ where

$$J(t) \equiv \int_{-\infty}^{\infty} dx \frac{\partial \sigma}{\partial t}\frac{\partial \sigma}{\partial X} = M_X(R)\dot{X} \equiv P_X(t). \quad (16)$$

In the same manner we obtain the equations of motion for $\ddot{R}$; i.e., we multiply Eq. (1) by $\partial\sigma/\partial R$ and integrate over x. The result given in Eq. (3.19) of Ref. [6] is

$$\frac{d}{dt}[M_R(1-b_R)\dot{R}] = -\frac{\partial V_{\mathrm{eff}}}{\partial R} + 2\langle \sigma_{RR}|\partial\chi/\partial t\rangle \dot{R} - \beta M_R \dot{R}, \quad (17)$$

where

$$\frac{\partial V_{\mathrm{eff}}}{\partial R} \equiv \frac{\partial v_{\mathcal{R}}(R)}{\partial R} + \frac{\partial v_{\mathrm{dress}}(R)}{\partial R} - \frac{1}{2}\dot{R}^2\frac{\partial M_R}{\partial R}, \quad (18)$$

$M_R(R)=8[1-2R/\sinh 2R]$, and $b_R \equiv (M_R)^{-1}\langle \sigma_{RR}|\chi\rangle$ so that

$$-\dot{R}\frac{d}{dt}(M_R b_R) = -\dot{R}\langle \sigma_{RR}|\partial\chi/\partial t\rangle. \quad (19)$$

$v_{\mathcal{R}}(R)$ and $v_{\mathrm{dress}}(R)$ are defined in Eqs. (21) and (22), respectively. When we substitute Eq. (19) into Eq. (17) we obtain

$$\frac{d}{dt}[M_R(R)\dot{R}] \equiv \frac{d}{dt}P_R(R,t) = -\frac{\partial V_{\mathrm{eff}}}{\partial R} + 2\langle \sigma_{RR}|\partial\chi/\partial t\rangle\dot{R} - \beta M_R\dot{R}, \quad (20)$$

where the momentum conjugate to R is $P_R = M_R\dot{R}$ and where

$$v_{\mathcal{R}}(R) = 8\left[1 + \frac{\tanh^2\mathcal{R}}{\tanh^2 R} + 2R\left(\frac{1}{\sinh^2 R} + \frac{\coth R}{\cosh^2\mathcal{R}} - \frac{\tanh^2\mathcal{R}\cosh R}{2\sinh^2 R}\right)\right]. \quad (21)$$

Figure 2 shows $v_{\mathcal{R}}(R)$ as a function of R for $\mathcal{R}=0.24$. The force on $R(t)$ due to the phonon dressing is

$$\frac{\partial v_{\mathrm{dress}}(R)}{\partial R} = -\frac{16}{\pi}f\left[\int_{-\infty}^{\infty} d\mu\, \mathrm{sech}^2(2R-\mu)\tanh(2R-\mu) \times \mathrm{sech}\,\mu\tanh\mu - \int_{-\infty}^{\infty} d\mu\,\mathrm{sech}^2(2\mathcal{R}-\mu) \times \tanh(2\mathcal{R}-\mu)\mathrm{sech}\,\mu\tanh\mu\right]. \quad (22)$$

Note that $\partial v_{\mathrm{dress}}(R)/\partial R$ vanishes at $R=\mathcal{R}$ as does $v_{\mathcal{R}}(R)$. The terms $\langle\sigma'|\chi'\rangle$ and $\langle\sigma'_R|\chi'\rangle$ in Eq. (15) and the terms $\partial v_{\mathrm{dress}}(R)/\partial R$ and $\langle\sigma_{RR}|\chi\rangle$ are first order in ϵ_1 and ϵ_2. Since we have solved for χ to only first order in ϵ_1 and ϵ_2, it is sufficient to evaluate these four terms with $R(t)-\mathcal{R}_{\min}$ where $\mathcal{R}_{\min}$ is the minimum of $v_{\mathcal{R}}(R)$ which occurs at $R=\mathcal{R}$. In this paper we take $\mathcal{R}_{\min}=2.4$. At $R=\mathcal{R}$ the force $\partial v_{\mathrm{dress}}(R)/\partial R=0$.

Consequently we expand $\partial v_{\mathrm{dress}}(R)/\partial R$ to first order in $R-\mathcal{R}$ which yields

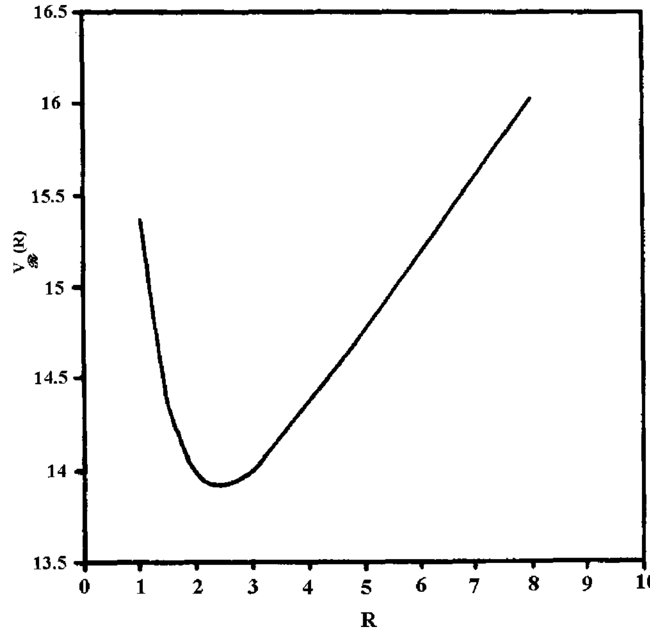

FIG. 2. The effective nonlinear potential $v_{\mathcal{R}}$ for $\mathcal{R}=0.24$.

$$\frac{\partial v_{\mathrm{dress}}(R)}{\partial R} = f\frac{16}{\pi}(R-2.4)\int_{-\infty}^{\infty} d\mu\{2\,\mathrm{sech}^2(4.8-\mu) - 3\,\mathrm{sech}^4(4.8-\mu)\}\mathrm{sech}\,\mu\tanh\mu. \quad (23)$$

The values of the dot products evaluated at $R=\mathcal{R}=2.4$ are $\langle\sigma'|\partial\chi'/\partial t\rangle=0.025\dot{f}$, $\langle\sigma'_R|\chi'\rangle=0.0242f$, $\langle\sigma_{RR}|\partial\chi/\partial t\rangle=0.05\dot{f}$, and $\partial v_{\mathrm{dress}}(R)/\partial R=-0.115f(R-2.4)$.

Finally, the coupled equations of motion for $\ddot{X}$ and $\ddot{R}$ are

$$\frac{d}{dt}[M_X(R)\dot{X}] + \beta M_X(R)\dot{X} - 4\pi f_1 = f\left\{-0.1275\frac{\dot{f}}{f} + 0.1232\dot{R}\right\}, \quad (24)$$

$$\frac{d}{dt}[M_R(R)\dot{R}] + \beta M_R(R)\dot{R} + \frac{\partial v_{\mathcal{R}}(R)}{\partial R} = \frac{1}{2}\dot{R}^2\frac{\partial M_R}{\partial R} + f\left\{-0.115(R-2.4) + 0.5097\frac{\dot{f}}{f}\dot{R}\right\}. \quad (25)$$

It is also useful to express Eqs. (24) and (25) in terms of the momentum

$$\frac{dP_X}{dt} + \beta P_X - 4\pi f_1 = fP_X(M_X)^{-1}\left\{0.1275\frac{\dot{f}}{f} + 0.1232\frac{P_R}{M_R}\right\}, \quad (26)$$

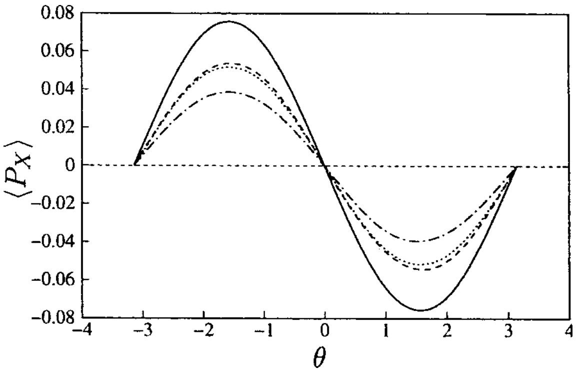

FIG. 3. This figure demonstrates symmetry breaking—i.e., the nonvanishing of $\langle P_X(t)\rangle$ as a function of θ for various values of the parameters ω, ϵ, and β. Solid curve: $\omega=0.05$, $\epsilon_1=\epsilon_2=0.03$, and $\beta=0$ (the curve is multiplied by 0.02). Dashed curve: $\omega=0.15$, $\epsilon_1=0.3$, $\epsilon_2=\epsilon_1/\sqrt{3}$, and $\beta=0.2$. Dotted curve: $\omega=0.125$, $\epsilon_1=0.16$, $\epsilon_2=\epsilon_1/\sqrt{2}$, and $\beta=0.15$. Dash-dotted curve: $\omega=0.05$, $\epsilon_1=\epsilon_2=0.05$, and $\beta=0.12$.

$$\frac{dP_R}{dt}+\beta P_R-\frac{P_R^2}{2M_R^2}\frac{\partial M_R}{\partial R}+\frac{\partial v_{\mathcal{R}}(R)}{\partial R} = f\left\{0.115(R-2.4)+0.5097\frac{\dot{f}}{f}\frac{P_R}{M_R}\right\}. \quad (27)$$

Note that the right-hand sides of the above equations are proportional to the phonon dressing—i.e., f.

Before proceeding to the results of simulations in the next section we make a few observations about the coupled equations of motion for $\ddot{X}$ and $\ddot{R}$. The equation of motion for $\ddot{X}$ has a steady-state solution because the ac driver $4\pi f_1(t)$ is able to balance the damping due to the reservoir $\beta M_X\dot{X}$. The absence of the phonon dressing χ—i.e., f in Eq. (26) for $\ddot{R}$—has the consequence that $R(t)$ would not see the ac driver at all and the reservoir damping due to the reservoir $\beta M_R\dot{R}$ would cause $R(t)$ to decay to the minimum of $v_{\mathcal{R}}(R)$ which is at $R=\mathcal{R}$ and there would then be no time dependent internal mode. Consequently there would be no persistent energy current; i.e., $\langle P_X(t)\rangle$ would vanish. Equations (26) and (27) satisfy time inversion symmetry when $\beta=0$ and $\theta=0\pm n\pi$.

III. RESULTS OF SIMULATIONS

In this section we present the results of computer solutions of Eq. (26) for $P_X(t)$, of Eq. (27) for $R(t)$, and for the time average of the energy current, $J(t)$, which is equal to the time average of $P_X(t)$ because, from Eq. (16), $J(t)=P_X(t)$. The definition of the time average is $\langle P_X(t)\rangle \equiv \lim_{T\to\infty}(1/2T)\int_{-T}^{T}dt'\,P_X(t')$. In Figs. 3 and 4 we present the results for $\langle P_X(t)\rangle$ for a range of values of ω, ϵ_1, ϵ_2, and β which clearly show the persistent energy current as a function of θ including the Hamiltonian limit where $\beta=0$. At $\theta=0\pm n\pi$ the ac driver is shift symmetric, so there is no symmetry breaking for $\beta=0$ and for $\beta\neq 0$ the shift symmetry is only approximately satisfied becoming exact as $\beta\to 0$. At all other θ the ac driver is not shift symmetric and we have symmetry breaking of the energy current for the DSG just as we did in Ref. [4] for the SG. In Figs. 5 and 6 we have typical examples of computer solutions for the CV's $R(t)$ and $P_X(t)$ for various values of the parameters ω, β, ϵ_1, and ϵ_2. In both figures we see that $R(t)$ behaves as the solution of the equation of motion for a point particle moving in a single minimum asymmetric potential well, driven by a two-frequency driver. The momentum conjugate to $X(t)$, behaves like the momentum of a damped point particle weakly coupled to R and driven by a two-frequency ac driver.

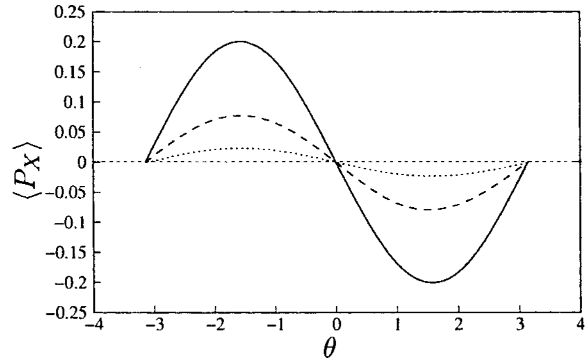

FIG. 4. $\langle P_X(t)\rangle$ as a function of θ for $\omega=0.05$, $\epsilon_1=\epsilon_2=0.03$ for various values of β shows a monotonic decrease of the amplitude of $\langle P(t)\rangle$ as the damping β increases. Solid curve: $\beta=0.02$. Dashed curve: $\beta=0.05$. Dotted curve: $\beta=0.12$.

IV. DISCUSSION

We chose the internal variable $R(t)$ to be the internal variable for symmetry breaking in the DSG. We equally well could have chosen the internal variable for symmetry breaking to be $\Gamma(t)$. Either $R(t)$ or $\Gamma(t)$ or both will cause symmetry breaking in the DSG, whereas in the SG case the only

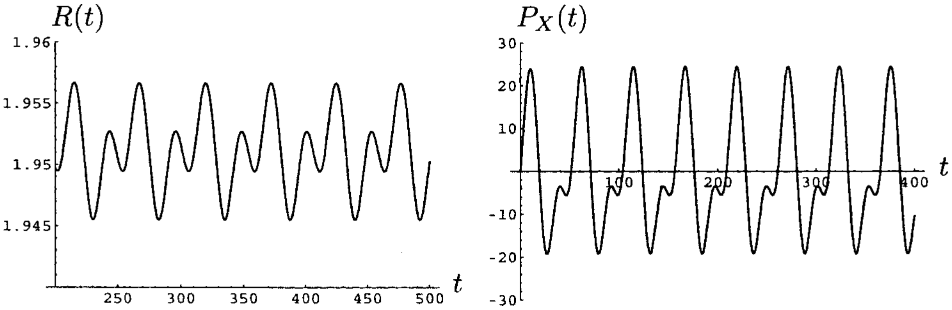

FIG. 5. The energy current $P_X(t)$ and the distance between the subkinks of the DSG, $R(t)$, for the parameters $\beta=0.1$, $\epsilon_1=\epsilon_2=0.2$, $\theta=1.61-\pi$, and $\omega=0.12$.

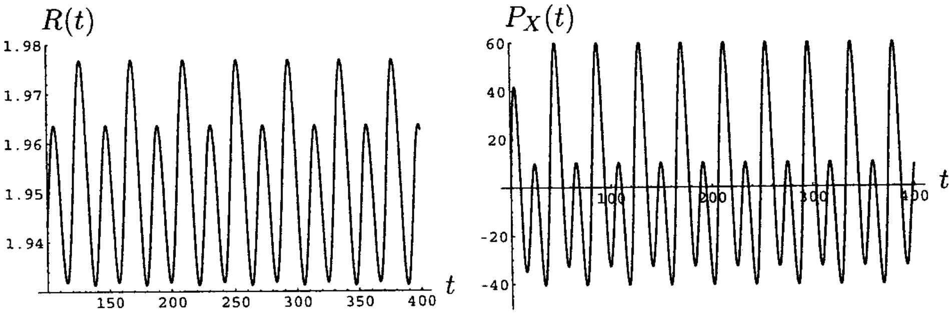

FIG. 6. $P_X(t)$ and $R(t)$ for the parameters $\beta=0.2$, $\epsilon_1=0.5$, $\epsilon_2=1$, $\theta=0$, and $\omega=0.15$. Both curves show the effect of two driving frequencies. The time average of $P(t)$ is nonzero and $R(t)$ has a two-frequency nonlinear oscillation about the minimum of the asymmetric potential well.

internal variable possible is $\Gamma(t)$. In all cases there can be no symmetry breaking unless the phonon dressing caused by the ac driver is included in the equations of motion. This can be seen clearly in Eq. (24) where if $\chi=0$ (i.e., $f=0$) the equation of motion for the energy current is

$$\frac{dP_X}{dt} + \beta P_X = 4\pi f_1. \tag{28}$$

The infinite time average of the energy current is $\langle P_X(t)\rangle =0$ and thus there is no directed energy current; i.e., time inversion symmetry is not broken if $\chi=0$. We showed in Ref. [4] that if the dressing χ vanished then $\langle P_X(t)\rangle=0$. Thus the necessary condition for a directed energy in both the SG and DSG equations is that the phonon dressing $\chi(t)$ be nonzero.

Recently, in Ref. [7], a very different generalized double sine-Gordon that has a spatially asymmetric potential, which is driven by a single-frequency ac driver, was used to obtain spatial ratchet behavior. Their spatial symmetry breaking mechanism with a single-frequency ac driver is completely different than our spatially symmetric DSG with a two-frequency ac driver which violates time shift symmetry.

[1] S. Flach, Y. Zolotaryuk, A. E. Miroshnichenko, and M. V. Fistul, Phys. Rev. Lett. **88**, 184101 (2002).
[2] O. Yevtushenko, S. Flach, Y. Zolotaryuk, and A. A. Ovchinnikov, Europhys. Lett. **54**, 141 (2001).
[3] S. Flach, O. Yevtushenko, and Y. Zolotaryuk, Phys. Rev. Lett. **84**, 2358 (2000).
[4] C. R. Willis and M. Farzaneh, Phys. Rev. E **69**, 056612 (2004).
[5] C. R. Willis *et al.*, Phys. Rev. B **35**, 3496 (1987).
[6] R. Boesch, P. Stancioff, and C. R. Willis, Phys. Rev. B **38**, 6713 (1998), and references therein.
[7] M. Salerno and N. Quintero, Phys. Rev. E **65**, 025602R (2002).